DEVELOPMENT OF INSERTION DEVICES AT NSRRC

C. H. Chang, C. S. Hwang, T. C. Fan, F. Y. Lin, H. H. Chen, M. H. Huang, Ch. Wang
and J. R. Chen, NSRRC, Taiwan

Abstract

Five high-performance insertion devices are currently operated in the 1.5 GeV storage ring of the National Synchrotron Radiation Research Center (NSRRC). Four devices are conventional permanent magnet insertion devices and another is a 5 T superconducting wavelength shifter. This article presents the spectral characteristics and magnetic field quality of these devices. A 3.2 T superconducting wiggler (SW6) with a 6-cm period and 32 poles was recently installed in the down stream of the RF cavity. The construction and testing of the superconducting wiggler are also described. Moreover, three more superconducting wigglers are presently being fabricated to enhance the hard X-ray source. Additionally, a 1.5 T superconducting undulator with a period of 15-mm is being designed to provide high photon energy of between 400 eV and 5 KeV. This study also considers the feasibility of a superconducting helical undulator.

INTRODUCTION

The Taiwan Light Source is a third-generation 1.5 GeV energy synchrotron radiation source optimized to generate soft X-rays. The storage ring has four 6-m long straight sections for installing insertion devices. Presently, the W20 wiggler and the U5, the U9 and the EPU5.6 undulators are now in operation [1]. These are the four conventional permanent magnetic insertion devices. The demand for intensive hard X-rays has been recently increasing. At NSRRC lower energy storage ring, a 5 T compact superconducting wavelength shifter (SWLS) was installed between the two kicker magnets in the injection section and a 3.2 T superconducting wiggler was installed in downstream of the RF cavities section [2,3]. Table 1 lists the main parameters of these insertion devices.

Figure 1 compares the photon fluxes of various insertion devices with that of a bending magnet source. Superconducting insertion devices are used to extend operation into the harder X-ray region to promote the flux by a factor of ten at 10-20 K eV.

Figure 1: The photon fluxes of various insertion devices
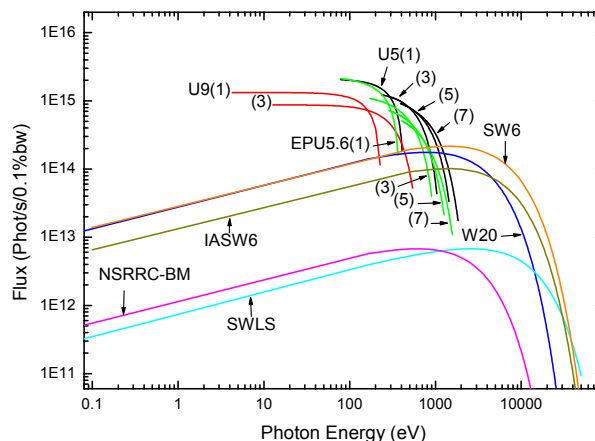
with that of a bending magnet source.

PERFORMANCE OF PERMANENT MAGNET UNDULATOR

Five high-performance conventional insertion devices were completed in 1999. These included a 2-m long U10 undulator and a 3.9-m long EPU5.6 elliptically polarizing undulator, which were designed and built at the NSRRC. W20, U5 and U9 are vendor–built insertion devices. The APPLL II type EPU5.6 undulator operates in various linear, elliptical and circular polarization modes [4]. The magnetic structure is optimized to achieve a higher peak field and a wider uniform field at a minimum gap width.

Table 1: The main parameters of the insertion devices

	W20	U10	U5	U9	EPU5.6	SWLS	SW6
Type	Hybrid	Hybrid	Hybrid	Hybrid	Pure	SC	SC
λ [cm]	20	10	5	9	5.6	32.56	6
Gap [mm]	22	22	18	18	18	56	18
N	13	20	76	48	66	1.5	32
Photon energy (keV)	4-15	----	0.06-1.5	0.004-0.5	0.06-1.5	4-33	6.5-19
Deflection K	33.6	9.34	2.99	10.5	3.5 (2.35)	----	17.9
Bmax. [T]	1.8	1.0	0.64	1.25	0.67 (0.45)	5	3.2
Phase error Θ	N/A	2.5°	3°	3.7°	5.5°	N/A	N/A
$\theta x (\theta y)$ [μrad]	N/A	15 (6)	6 (11)	20 (10)	10 (15)	N/A	N/A
$\delta x (\delta y)$ [μm]	N/A	5 (2)	7 (10)	8 (2)	2 (1)	N/A	N/A
Beam duct aperture(cm^2)	1.7x8	1.7x8	1.3x8	1.3x8	1.3x8	2.0x10	1.1x8
Installation	Dec.1994	Oct.1995	Mar.1997	Apr.1999	Sep.1999	Apr. 2002	Jan.2004

Magnet sorting and the shimming methods were implemented to improve the quality of the magnetic field. An insertion device must have zero or very low integrated multipoles on the axis of the electron beam to maintain the stability of the electron beam that circulates in the storage ring. Multipole shimming eliminates the field errors in all conventional insertion devices. Figure 2 plots the horizontal and vertical field integrals in the minimal gap between these undulators after shimming. The flatness of curves as a function of the transverse axis reveals very low multipoles. Figure 3 presents the on-axis first field integrals versus the gap change. Both field integral errors are below 30 G-cm at any magnetic gap. Spectral shimming reduces the phase errors within 5° allowing almost ideal spectral performance at the high harmonics. The horizontal and vertical close orbit distortions of these IDs are approximately 0.2 to 0.3 mm without correction implying. It revealed the main vertical and horizontal field errors within a small field tolerance. Furthermore, the distortion of the electron orbit can be reduced to within a few microns with a feed forward table if only one ID gap varies at one time. The peak real-time orbit distortion exceeds 10 microns in the ID's field scan. Moreover, a fast digital orbit feedback system was applied, and the peak orbit maintained within a few microns [5].
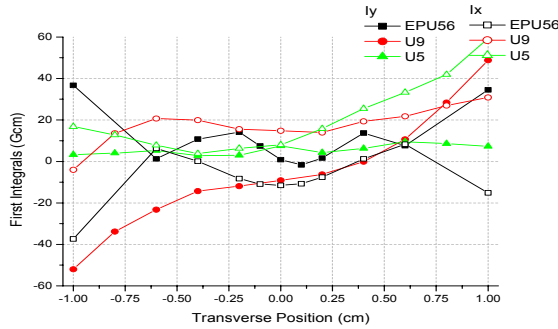
Figure 2: The horizontal and vertical field integrals as a function of the transverse axis
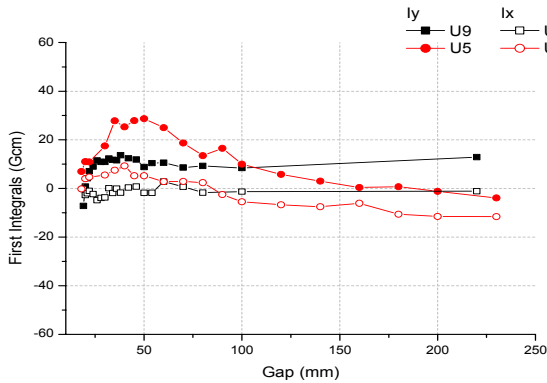
Figure 3: The on-axis first field integrals versus the gap change.

TESTS OF SUPERCONDUCTING WIGGLERS

The high demand for X-ray has been increasing. The superconducting wiggler extends the range of accessible photon energies. A compact 5T superconducting wavelength shifter and a 3.2 T superconducting wiggler are now installed in the storage ring. The SWLS magnet can extend the critical photon energy from 2.14 keV to 9 keV as the flux increases. Table 2 presents the main parameters of the superconducting magnet. Three pairs of racetrack superconducting coils were designed to generate the central field strength of 6 T, and to modify the integral field close to zero. The shapes of pole and the superconducting coils are designed to minimize the higher harmonic terms of the magnetic field, and especially the sextupole field component.

The wavelength shifter has a warm beam duct, which is 600 mm long and 100 mm wide with a gap of 20 mm. The beam aperture is required to prevent heating by photon radiation. The SWLS magnet is regularly cooled using a single 1.5 W Gifford-McMahon cryocooler. Additionally, a 50-l liquid helium vessel and a 15-l liquid nitrogen reservoir are used initially to cool the magnet and provide emergency backup. An S-shaped flexible copper plate is used to connect the cold head of the cryocooler to the superconducting coils to dampen the vibrations.

Table 2: The main parameters of the superconducting magnet.

	SW6	IASW6	IVSU1.5
B_{max} (T)	3.2	3.2	1.5
λ (cm)	6.0	6.0	1.5
Pole gap (mm)	18	19	5
Eff. Pole No.	28	13	117
Beam duct aperture (mm²)	8 0x 11	100 x 11	100 x 5
Parameter k	17.9	17.9	2.1
Cooling type	LHe	LHe	LHe

A superconducting wiggler was installed in downstream of the RF cavity section in January 2004. The superconducting wiggler has 32 pairs of racetrack NbTi superconducting coils with a periodic length of 60 mm, generating a magnetic field strength of 3.2 T at gap width of 18-mm [6]. The SW6 magnet produces ten times more photon flux at 10 keV than the present SWLS device in the X-ray beamline.

The cryostat is designed to minimize the transfer of heat by radiation and conduction from the ambient to the cold mass. The magnet is operated in a 4.2 K liquid helium vessel. An ultra-high vacuum (UHV) bean tube is an integral part of the cryostat and is thermally intercepted in a liquid nitrogen reservoir at 77 K. However, the UHV aluminum chamber is completely isolated from the cryostat vacuum. An aluminum chamber

is chosen because of its good thermal conduction. Figure 4 schematically depicts the UHV chamber and the 4.2 K duct. Poles and coils are assembled in an aluminum block in the top and bottom halves of magnetic array, respectively. An Al bar used to separate magnets maintains a gap of exactly 18-mm between the top and bottom magnet arrays. A minimum aperture of 11 mm is required for beam dynamics. Thermal shielding leaves only 1mm clearance between the magnetic cold mass at 4.2 K and the UHV vacuum chamber at 77 K. Fiberglass bumpers were inserted to prevent thermal conduction during the cooling-down of the magnet. A bimetal vacuum duct was welded between the Al vacuum beam duct and the thermal expansion bellow at both short ends. Thermal analysis was performed using ANSYS computer code to determine the distributions of temperature on the vacuum chamber at 77 K.
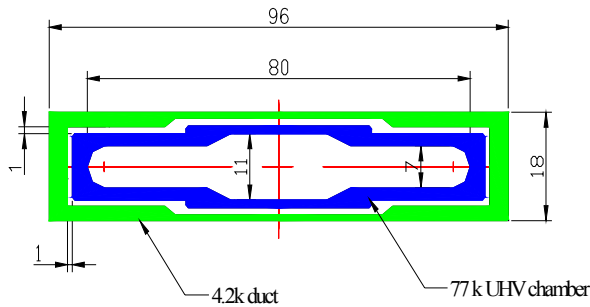
Figure 4: Schematically depicts the UHV chamber and the 4.2 K duct.

The magnetic measurements must be sufficiently precise, accurate and reliable to enable the quality of the field of the superconducting insertion devices to be determined. The SW6 was fully tested and detailed field profiles were obtained in the vertical testing 4.2 K dewar [7]. The main power supply charges all 32 coils in series to generate the nominal peak field. Two trim power supplies are connected to the two first-end pole coils, respectively, to eliminate the first and second field integrals. The SW6 is also fully tested in the cryostat. A Hall probe must be inserted into a flat warm bore chamber to take detailed field measurements in the small gap at room temperature. Figure 5 shows the first and second integral field distributions in the longitudinal

direction following the end pole optimization. The performance and stability of all systems were evaluated. The SW6 wiggler chamber with an 11-mm aperture was successfully tested; it does not degrade the vacuum of the ring.

When all ID straight sections are already occupied, no insertion device can be installed in another long straight section. The possibility of installing short insertion devices into achromatic sections of the machine lattice has been studied to increase the number of insertion devices in the storage ring. An in achromatic superconducting wiggler (IASW6) with a maximum length of 1 m is designed, as shown in Fig. 6, because space between the bending magnet is limited. A 15-pole compact superconducting wiggler with a periodic length of 6 cm is designed. This wiggler magnet with a maximum peak field of 3.1 T at a pole gap width of 19 mm is operated in the 4.2 K liquid helium vessel. A five-pole prototype magnet is tested and measured to confirm its magnetic field performance in the test dewar. Irradiation from IASW6 and the bending magnet hits the vacuum chamber downstream. A 120-mm wide vacuum chamber prevents heating by the photon irradiation. Cryogenic considerations are incorporated into the thermal analysis of the wiggler magnet and the 77 K cold bore vacuum chamber.
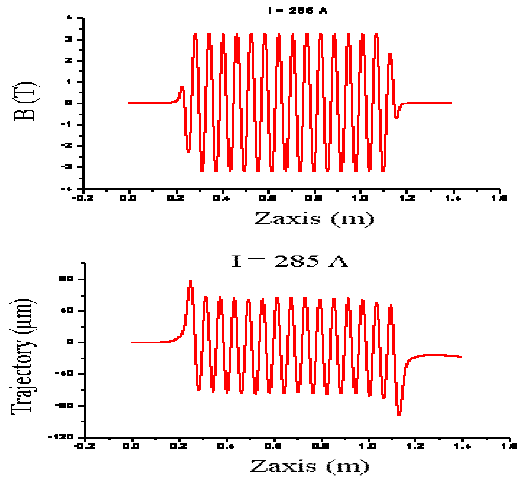
Figure 5: The first and second integral field distributions in the longitudinal direction.
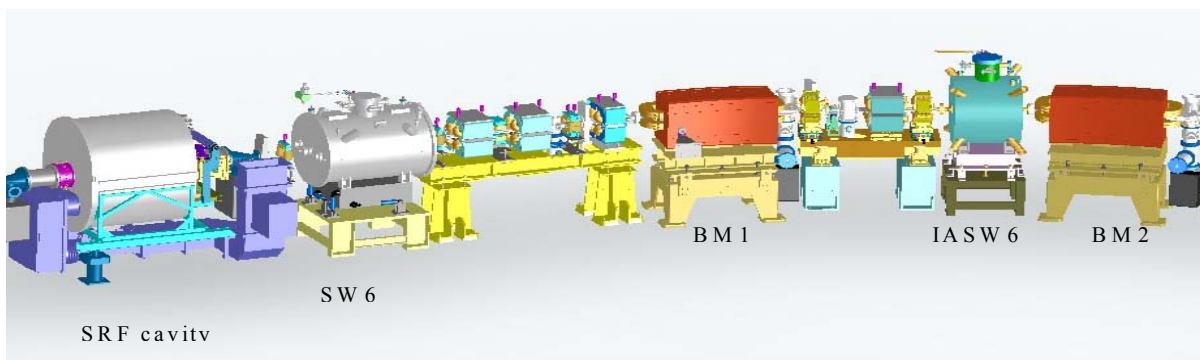
Figure 6: Design of in achromatic superconducting wiggler (IASW6) with a maximum length of 1 m

Five superconducting magnets will be completed in 2006 to improve the performance of the storage ring and extend the X-ray source. Additional superconducting undulators are being developed. An independent 400 W cryogenic plant for the superconducting insertion devices is presently begun built. The cryogenic transfer line with control valves in a circle with a 120-m circumference. A distribution valve box is connected to backup the superconducting RF cryogenic system.

ONGOING R&D OF SUPERCONDUCTING UNDULATOR

An important goal is to reduce the magnetic gap to increase the magnetic field strength. The limiting magnetic gap affects the lifetime and injection efficiency of the electron beam. Top-up mode injection was tested to measure the minimum gap at 7 mm without reducing the efficiency of injection. Accordingly, an in-vacuo superconducting undulator has been studied for enhance the X-ray source in the 1.5 GeV storage ring [8]. A vertically wound racetrack coil structure with a periodic length of 15 mm provided photon energies of between 0.4 and 5 keV. Figure 7 plots the calculated field that corresponds to of the optimal magnetic flux density, and the first and second field integrals at a periodic length of 15 mm.
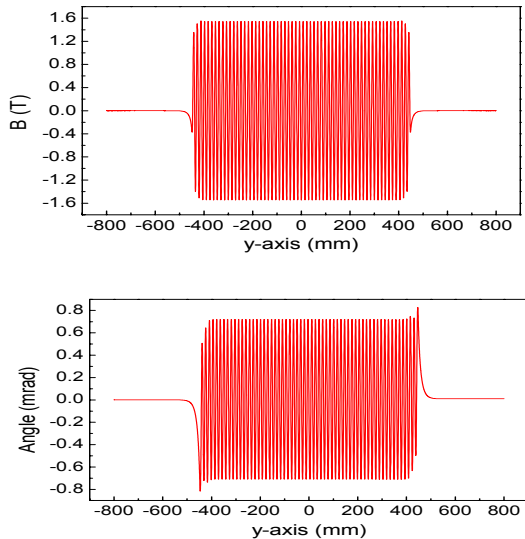
Figure 7: The calculated field that corresponds to of the optimal magnetic flux density, and the first and second field integrals at a periodic length of 15 mm.

A planar superconducting helical undulator was used to produce circularly polarized X-rays [9]. When the top and bottom magnetic pole arrays with alternative directions rotated wires and poles in the horizontal plane, as presented in Fig. 8, a helical field was generated, radiating circularly polarized light in the storage ring. Figure 9 the calculated field distributions in the longitudinal direction. Meanwhile, these two undulators with oppositely rotated wires and poles can perform a fast

switching of the right and left circularly polarized radiation.

Given a periodic length of 15.5 mm and a gap of 5 mm, the maximum magnetic flux densities in the helical undulator are $B_z=1.5$ T and $B_x=1.2$ T when the wires are rotated by 60°. The roll-off $\Delta B/B$ considerably increases with increasing the angle rotation of the arrays of magnetic poles. The uniformity of the magnetic field affects the stability of the electron beam and reduces the size of the dynamic aperture. The merit flux of $P^2\varphi$ is regarded as a function of the angle θ in the two undulators, then the maximum merit flux is obtained at an angle of the rotation of 40° on the first harmonic spectrum. Hence, an angle of rotation of 20° is selected to obtain a favorable trade-off between the merit flux of all harmonic spectra and the effect of magnetic field on the electron beam.
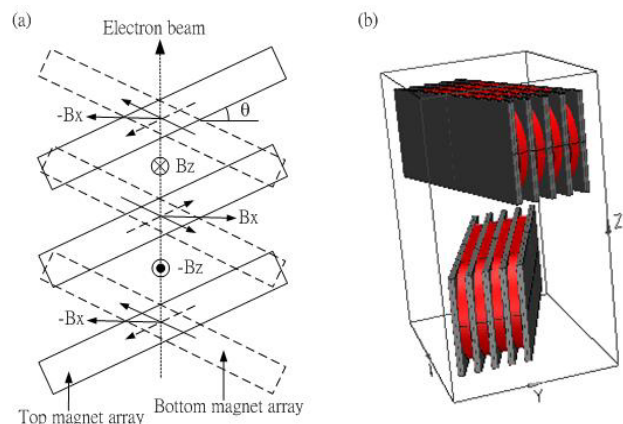
Figure 8: The superconducting helical undulator
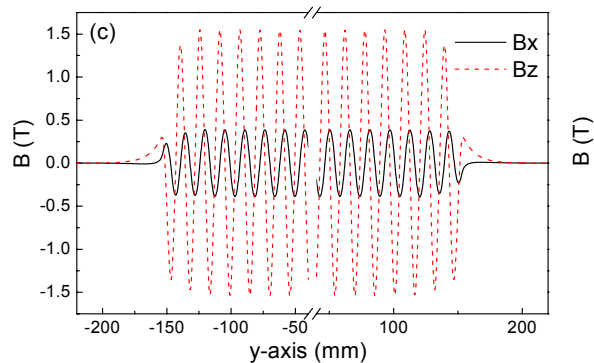
Figure 9: The calculated field distributions in the longitudinal direction.

CONCLUSIONS

Five high-performance insertion devices are routinely operated and provide versatile light sources for users. A 3.2 T superconducting wiggler with an 11-mm gap width has been installed in the storage ring. More than three superconducting magnets will be completed in 2006, greatly increasing the flux of X-rays, especially at photon

energies of over 10 KeV in the 1.5 GeV low-energy ring. A top-up mode injection was tested in the storage ring. An advanced in-vacuo superconducting undulator was developed to enhance the linear and circular polarization of X-rays. These insertion devices are expected to promote significantly the performance of the accelerator and provide an advanced high flux X-ray photon source.

ACKNOWLEGMENT

REFERENCES

[1] C. S. Hwang et al., "An overview of the insertion device development at SRRC" Nucl. Instr. and Meth. A 467-468 (2001) 114 – 117.

[2] C. S. Hwang et al., "Superconducting insertion devices for synchrotron hard x-ray at SRRC" in Proceeding of EPAC2002, 2002, pp. 2613-2615.

[3] C. S. Hwang, et al., "Design and construction performance of a compact cryo-free superconducting wavelength shiftre" IEEE Trans. On Appl. Supercon. VOL. 12, No. 1 2002, pp.686-690

[4] C. S. Hwang, et al., "Performance of an advanced elliptically polarized undulator undulator with shimming" RSI, March 2002, Vol. 73, No. 3, pp1436-1439

[5] H. P. Chang, C.H. Chang, et al., "Operational experience of the insertion devices and expectation of future superconducting wigglers at NSRRC" Oregon USA, May 12-16,PAC 2003

[6] C. S. Hwang, et al., "Design of a Superconducting Multipole Wiggler for Synchrotron Radiation" IEEE Trans. On Appl. Supercon. Vol.13, No. 2 2003

[7] T. C. Fan, et al., "Magnetic field measurement on superconducting multipole wiggler with narrow duct" Oregon USA, May 12-16, PAC 2003

[8] C. S. Hwang et al., "Comparison of Predesign Parameters for Mini-Pole In-Vacuo Superconducting Undulators" in Proceeding of MT-18, Japan, 2003

[9] C. S. Hwang, et al., "A superconducting helical undulator with fast switching circularly polarized light", NSRRC/MG/IR/Hwang-01-04